



HAL
open science

Multi-scale modelling of timber-frame structures under seismic loading

Clément Boudaud, Luc Davenne, Julien Baroth, Laurent Daudeville

► **To cite this version:**

Clément Boudaud, Luc Davenne, Julien Baroth, Laurent Daudeville. Multi-scale modelling of timber-frame structures under seismic loading. World Conference on Timber Engineering (WCTE 2014), Aug 2014, Québec, Canada. pp.1905-1911. hal-02004479

HAL Id: hal-02004479

<https://hal.science/hal-02004479>

Submitted on 30 Jun 2024

HAL is a multi-disciplinary open access archive for the deposit and dissemination of scientific research documents, whether they are published or not. The documents may come from teaching and research institutions in France or abroad, or from public or private research centers.

L'archive ouverte pluridisciplinaire **HAL**, est destinée au dépôt et à la diffusion de documents scientifiques de niveau recherche, publiés ou non, émanant des établissements d'enseignement et de recherche français ou étrangers, des laboratoires publics ou privés.

MULTI-SCALE MODELING OF TIMBER-FRAME STRUCTURES UNDER SEISMIC LOADING

Clément Boudaud¹, Luc Davenne², Julien Baroth³, Laurent Daudeville³

ABSTRACT: The proposed approach aims at developing tools to better predict the seismic vulnerability of timber-frame buildings. For such structures, the recent European code for design of earthquake resistant building (EC8 [1]) provides simplified methods which are considered relatively restrictive, especially concerning the design of roofs. EC8 also allows designers to carry on non-linear time history (dynamic) analysis for which numerical models capable of modeling different configurations of full structures are necessary. Timber frame structures are characterized by the use of metal fasteners (nails, screws, punched-plates, 3D connectors, etc.) in which dissipation phenomena are localized. The work presented herein consists in developing and validating a numerical model of wood-framed structures for dynamic calculations. The principle of the multi-scale approach, from the connections to the structure, was already proposed by Richard [2] or Xu [3]. It is now generalized to a large class of joints and validated at each scale, thanks to an important number of tests (more than 400 on joints, 25 on shear walls and 12 on roofs). Moreover, an improvement of the 1D hysteretic constitutive behaviour [4] is proposed to model dissymmetric behaviors and to model cumulative damages appearing under alternate loading. Eventually, a shake table test is performed on a 6 x 6 meters timber-frame house, and the results are confronted to the predictions of the numerical model of structure.

KEYWORDS: Timber-frame structures, Finite element, Cyclic and dynamic loading, Constitutive model, Macro-scale

1 INTRODUCTION

The study presented in this paper is motivated by two facts. Firstly, timber-frame construction is becoming a common building system in Europe. It presents many qualities, one of which being a good earthquake resistance due to both the excellent strength-to-density ratio of timber and the ductility of joints with metal fasteners, leading to limited inertia forces and providing good energy dissipation. Secondly, the recent European code for design of earthquake resistant buildings is accompanied in some countries by a new seismic hazard map. In France, based on this revised map, earthquake resistance calculations are now mandatory in a much larger part of the territory. Therefore, the seismic behavior of timber-frame structures has to be studied, in order to better understand their global and local behaviors.

Because nonlinear dissipative phenomena in timber-frame structures are mainly concentrated into metal connectors, simplified force-displacement models can be derived by fitting results of tests performed on joints. The proposed approach is based on a multi-scale concept, as proposed

previously by Richard et al. [2] or Xu et al. [3]. Such an approach requires a behavior law to represent the force-displacement evolution at each scale.

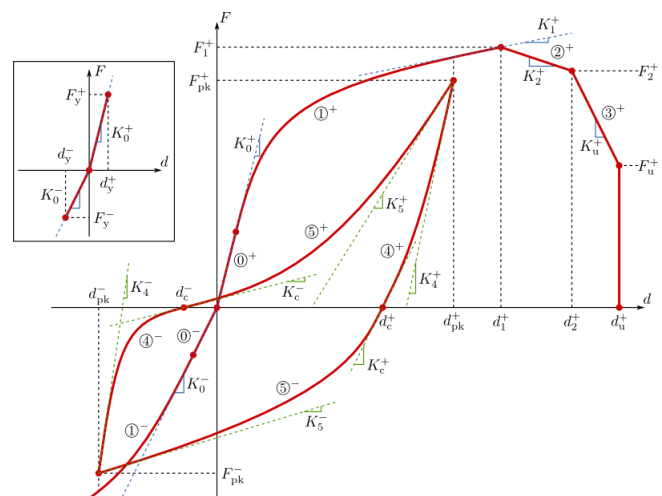


Figure 1: One-dimensional constitutive model used for the description of the force-displacement evolution at the scale of elementary joints or shear walls [4]

Numerous constitutive laws have been developed over the years (Ceccotti et al. [5], Folz et al. [6]). A new model, developed by Humbert et al. [4], can be considered as an

¹ LUNAM Univ., Groupe Ecole Supérieure du Bois, Nantes, France. Email: clement.boudaud@ecoledubois.fr

² Université Paris Ouest Nanterre la Défense, LEME, Ville d'Avray, France.

³ Univ. Grenoble Alpes, 3SR, F-38000 Grenoble, France. CNRS, 3SR, F-38000, France. Emails: firstname.name@3sr-grenoble.fr

improvement of Richard et al. [7] and Yasumura [8] models. It fulfils the needs of modeling asymmetric behaviors and cumulative damages appearing under alternate loading, and also provides a strict numerical continuity by using Bézier polynomials instead of commonly used exponential functions. This one-dimensional constitutive model is shown in Figure 1 and its parameters are listed in tables 1, 2 and 3.

Table 1: Model parameters governing the constitutive behaviour under monotonic loading

Parameter	Unit	Description
K_0	N/m	Initial elastic stiffness
d_y	m	Yield limit
d_1	m	Displacement at peak force
F_1	N	Peak force
K_1	N/m	Pre-peak tangent stiffness
d_2	m	Intermediate displacement limit
F_2	N	Force at intermediate limit d_2
d_u	m	Ultimate displacement
F_u	N	Force at ultimate displacement

Table 2: Model parameters governing the shape of the hysteresis loops

Parameter	Unit	Description
C_1	-	Unloading stiffness
C_2	-	Reloading stiffness
C_3	-	Tangent stiffness at $F=0$
C_4	-	Residual displacement

Table 3: Model parameters governing the damage indicator calculation

Parameter	Unit	Description
B_C	-	Linear coefficient of the DLF
B_R	-	Power term of the DLF
η	%	Damage proportion at constant amplitude cycles

DLF: Damage Limit Function

2 COUPLED EXPERIMENTAL- NUMERICAL APPROACH

2.1 SCALE 1: JOINTS

2.1.1 Experimental tests

More than 400 experimental tests on joints with metal fasteners were performed to provide input data for the numerical models of structural elements. Tests were performed under monotonic and cyclic loading following the protocol of the EN 12512 [9]. Tests were also repeated two or three times for monotonic loadings and five times

for cyclic loadings. Four different joints were tested: sheathing connections in shear walls (Figure 2.a), frame to frame connections in shear walls (Figure 2.b), punched metal plates in roof trusses (Figure 2.c) and 3D bracket type connectors (Figure 2.d) used to assemble the roof trusses on the walls. More details on the achievement and the results of these tests can be found in Humbert et al. [4].

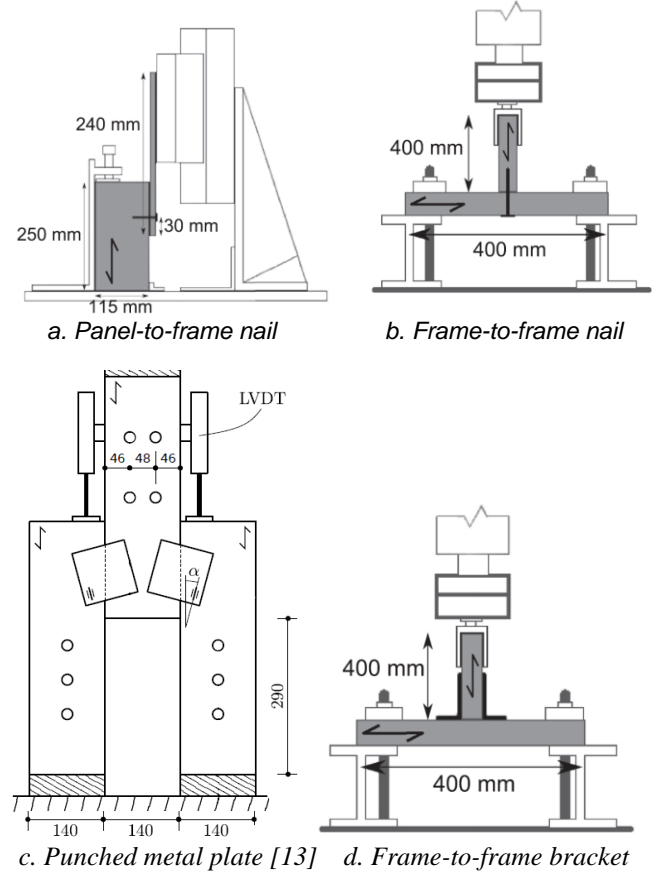


Figure 2: Experimental tests on metal fastened joints

2.1.2 Law calibration

The results of the tests are used to calibrate the one-dimensional constitutive model as shown in Figure 3. This model is based on 9 parameters that govern the behavior under monotonic loading (backbone curve) and 7 for the behavior under cyclic loading (Tables 1, 2 and 3). Two levels of calibration are distinguished. The first level is a direct calibration, which consists in reproducing one particular test. The second level is an average calibration, which consists in calibrating the parameters to reproduce the average behavior of several experiments.

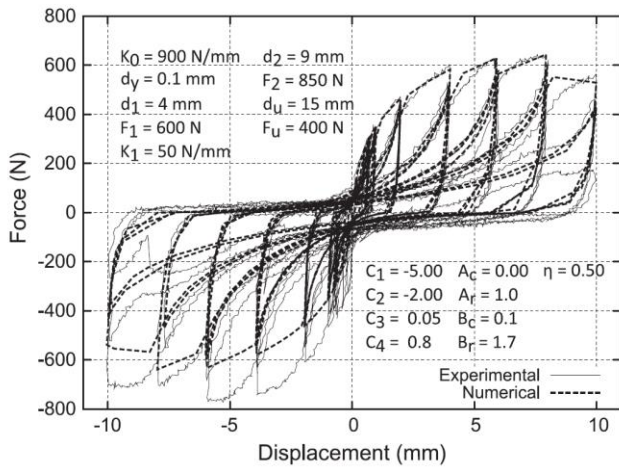


Figure 3: Direct calibration of a nailed joint (sheathing to framing connection) [4]

2.2 SCALE 2: STRUCTURAL ELEMENTS

2.2.1 Experimental tests

Several configurations of common 2.4 x 2.4 meters shear walls (Figure 4) were used to obtain the experimental behavior of shear walls under quasi-static (monotonic and cyclic) and dynamic (shake table) loadings, for a total of respectively 14 and 11 tests.

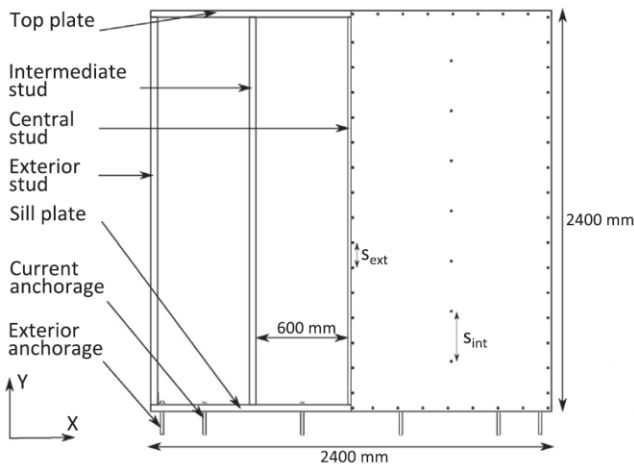


Figure 4: Shear wall description

Figure 5 presents the setup for a shear wall test on the shaking table of the Technological Institute FCBA in Bordeaux, France. The mass applied on the top of the shear wall intends to simulate the dead load due to the roof and an upper story. Depending on the test, the mass was 1500 or 2000 kg.

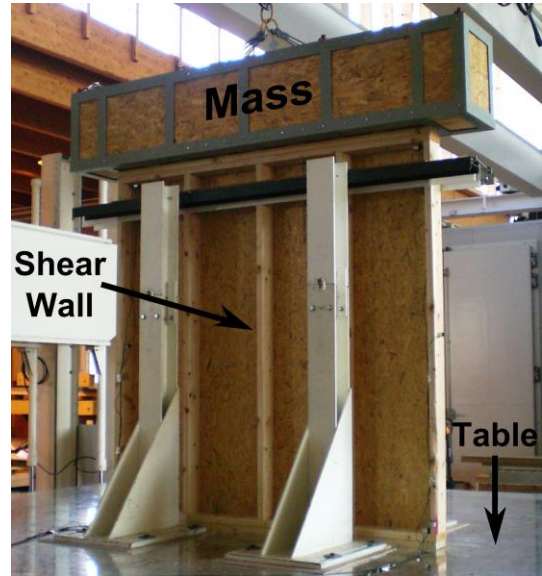


Figure 5: Shear wall setup for dynamic test

6 x 6 meters roofs were tested dynamically, for a total of 12 tests. Figure 6 shows a roof installed on the shaking table. As the table is only unidirectional, two tests were performed on each configuration of roof, with the roof trusses respectively parallel and perpendicular to the loading direction.



Figure 6: Roof setup for dynamic test

2.2.2 Numerical modeling

A detailed FE model of shear walls is developed using beam elements for the frame, plate elements for the panels and two-node spring-like finite elements for the joints. Figure 7 displays an exploded view of the mesh for a better understanding. The behaviors of joints have been identified at scale 1, k_n , k_s , k_f represent the non-linear stiffness of the joints. A detailed FE model of the roof is developed using the same approach.

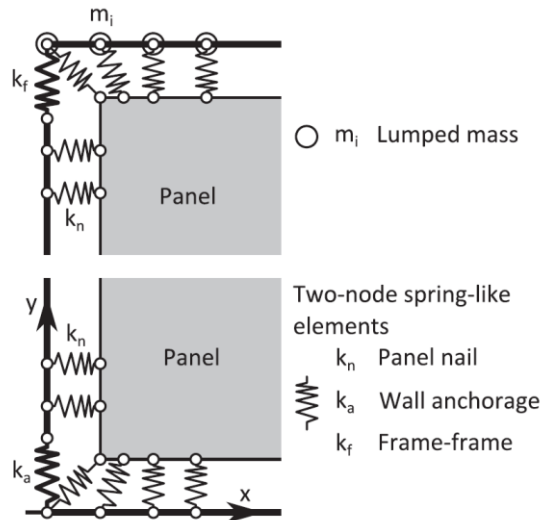


Figure 7: Finite element modeling of a shear wall

Figure 8 presents a comparison between an experimental result and the corresponding numerical prediction for a shear wall with OSB panels. It can be seen that the model predictions are in good agreement with the experimental behavior. Indeed, the pinching and peak forces of the hysteresis loops are in accordance with the experimental data. Over the 14 quasi-static tests, the average error of the numerical prediction of the peak force is 5 % [4].

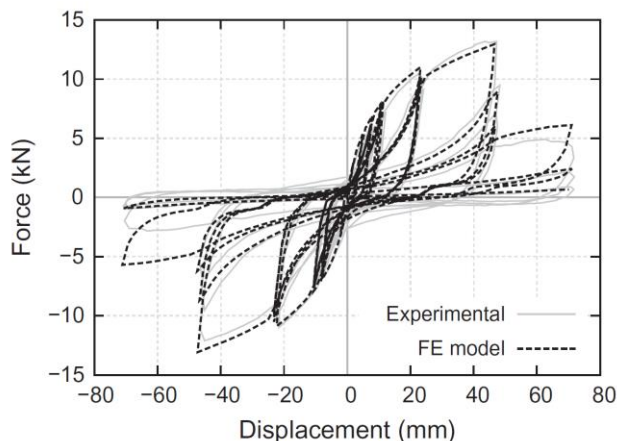


Figure 8: Comparison of experimental results and numerical predictions for a shear wall with 9 mm OSB panels [4]

A refined model of the roof was developed following the same modelling principles as the refined models of the shear walls.

Then, the shake table tests performed on the shear walls (11 tests) and the roofs (12 tests) were simulated. Figure 9 presents the comparison between experimental and numerical max and min relative displacements of the shear

walls for the 11 dynamic tests. Numerical predictions are more accurate for some tests than others, but on the whole the model is able to predict the behavior for different configurations of shear walls and different levels of loading. Similar work was achieved for roofs.

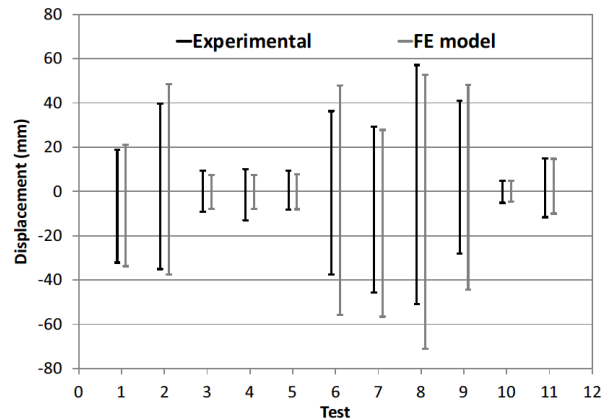


Figure 9: Comparison of experimental results and numerical predictions for a shear wall with 9 mm OSB panels [4]

Note that the modeling of the dynamical tests performed on shear walls and roofs was carried out by considering a viscous damping. A Rayleigh damping was considered i.e. the damping matrix is as a linear combination of the mass and stiffness matrices. The damping matrix is built by considering the two first modes. The damping ratio is identified using low amplitude free vibration responses after white noise solicitations. It is assumed that for relative displacement of the order of 1 mm, hysteretic damping does not occur. Based on the conclusions of Dutil and Symans [12], the logarithmic decrement method is used to calculate the damping ratio, rather than the bandwidth method based on the Frequency Response Function (FRF). For shear walls and roofs, the two identified ratios were 5 % and 2 % respectively.

2.3 SCALE 3: STRUCTURE

2.3.1 Experimental tests

A dynamic test has been performed on a single-story 6 x 6 meters timber-frame house (Figure 10). All three translational DOF of the shake table are submitted to ground motions corresponding to a severe seismic hazard. The scenario for Guadeloupe (French Caribbean Island) has been chosen. The most probable magnitude-distance couple was identified for this scenario and for a return period of 475 years (probability of exceedance of the peak ground acceleration of 10 % in 50 years). Seismic ground motion histories are represented Figure 11. The resulting peak ground acceleration is 0.33 g in Y-axis. These histories have been applied to the structure, considering a growing amplification coefficient. Resulting PGA are between 0.33 g (100%) to 0.99 g (300%).



Figure 10: Overview of the house on the shaking table

Experimental observations show that there is no torsion of the structure during the test. It was expected that the torsion would be small but observable, as one of the walls includes a wide opening of 2.8 m for a wall length of 6 m. This result is most certainly explained by the reinforcement of the roof, in order to behave like rigid diaphragm, which was in accordance with the French building regulations.

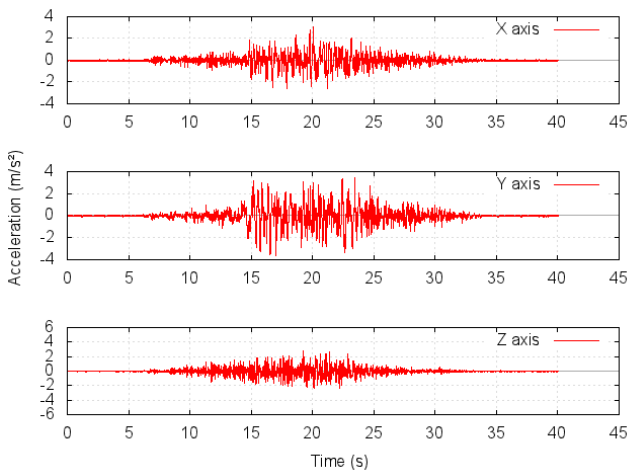


Figure 11: Ground motion histories corresponding to a severe seismic hazard (Guadeloupe, French Caribbean island) [5]

2.3.2 Numerical modeling

A detailed FE modeling of the whole timber-frame house is too time-consuming. Because of the particular parallelogram-like kinematics of the shear wall, it is proposed to consider the shear wall deformation by means of a simplified FE model consisting of a one degree of freedom moving frame (Figure 12). Shear wall kinematic is a combination of parallelogram-like deformation, overturning (due to uplift of the anchorage) and shear (Gupta and Kuo [11]). The simplified FE model only has

the parallelogram-like kinematic. Its nonlinear behaviour of the simplified FE model arises from the constitutive relationship used for the joints [4]. The parameters of this non-linear model were identified from the results of the refined FE model under both push-over and cyclic loadings. Therefore, the effect of overturning and shear are indirectly taken into account.

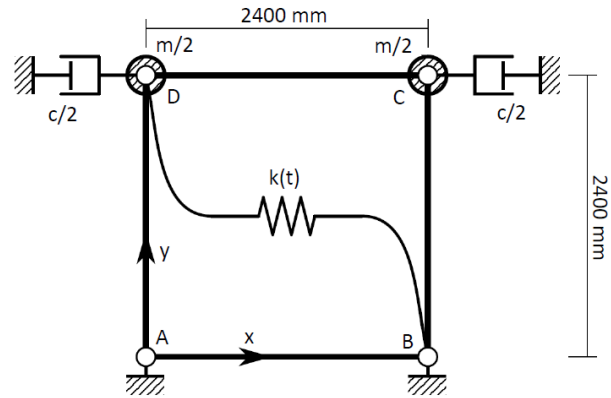


Figure 12: Simplified FE model of shear wall

The simplified FE model is calibrated for quasi-static loading and then used in dynamic calculations. To assess the accuracy of its behaviour under dynamic loading, the simplified FE model predictions and the experimental results under dynamic loading are compared. The results show a good agreement, validating the use of a single degree of freedom model using the developed constitutive behaviour law.

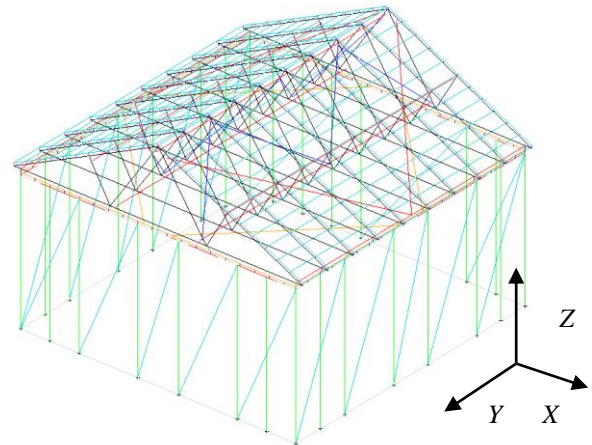


Figure 13: Overview of the finite element model of the house

The model of the structure is then built by assembling the simplified FE models of shear walls with kinematic relations, and eventually the detailed FE model of roof (Figure 13). The roof was attached to the simplified shear

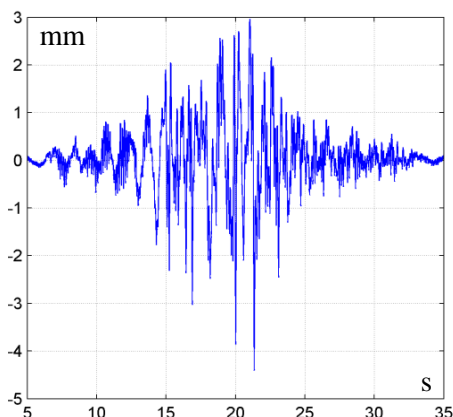
walls by spring-like elements that model the 3D bracket-type connectors.

In the following, only the nominal ground motion presented in Figure 11 is applied with 100 % and 200 % amplification coefficients (PGA respectively equal to 0.33 g and 0.66 g).

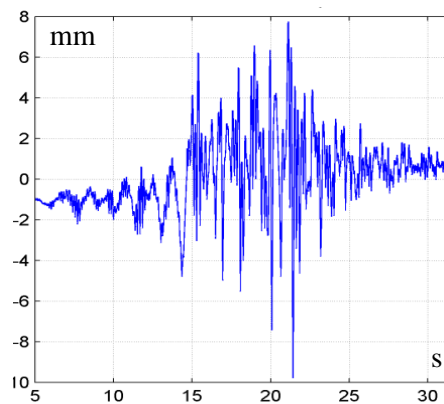
2.3.3 Results

One should note that the FE model predicts relative displacements at the top of the shear wall with the wide opening more important than those of the opposite wall. This induces a torsional effect on the structure that is not observed experimentally. The cause of that error between the experimentation and the model are currently ongoing research. Two possible causes are that the reinforcement of the roof might not be rigid enough, and that the wall to wall connections in the angles should transfer a resistive moment (this DOF was free for these calculations). The following comparison between experimental results and numerical predictions is made at the top of the shear wall opposite to the one with the wide opening.

Figure 14 depicts experimental top wall displacements for input ground motions with respectively 0.33 g (a) and 0.66 g (b) maximum peak ground accelerations (PGA).



a. Input loading with a 0.33 g PGA



b. Input loading with a 0.66 g PGA

Figure 14: Evolutions of top wall displacements from shake table tests

Figure 15 presents the model predictions in terms of peak displacements for the same input ground motions, considering that 0.33 and 0.66 g ground motions are applied consecutively in the same calculation (meaning that the 0.66 g solicitation is applied on the already damaged model after the 0.33 g loading).

Experimental and numerical histories are rather similar, with the same maximum displacements at same times: respectively around 4 and 10 mm for 0.33 and 0.66 g ground motions.

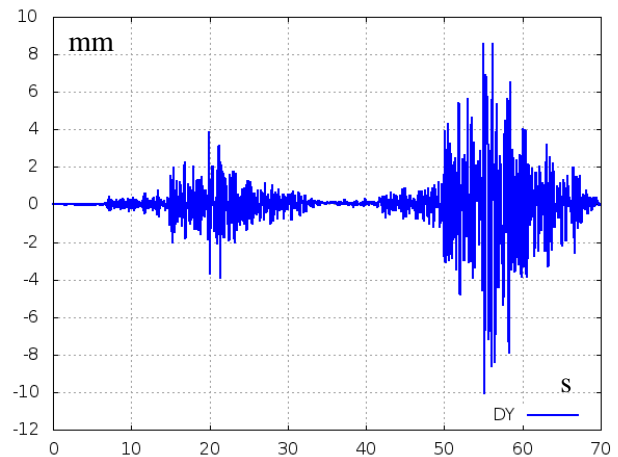


Figure 15: Evolutions of top wall displacements from FE simulations for 0.33 g and 0.66 g seismic loads

Table 4 presents relative displacements, between the top of walls and roofs and base of the structure. Computed and experimental values are compared. In this case, experimental values are slightly under-estimated by the numerical model.

Table 4: Computed and experimental average displacements at the top of walls and roofs

Peak ground acceleration	0.33 g		0.66 g	
	num	exp	num	exp
Wall/base (mm)	3.3	4.5	8.5	10
Roof/wall (mm)	2.8	4	6	6.5

2.3.4 Discussion

The presented results were obtained with a first blind simulation. Further analysis will be carried out.

The slight underestimation of displacements (Table 4) may be due to an overestimated damping (identified for both shear walls and roofs by means of shake table tests).

3 CONCLUSIONS

This study presents a numerical model of timber frame structure able to predict the nonlinear behavior under dynamic loadings. Using a multi-scale approach, from the elementary metallic joints to the structure, provides a computationally efficient and yet relatively accurate tool. More than 400 tests provide a large database of connectors' behavior and detailed FE models of structural elements are confronted to 14 quasi-static and 11 dynamic tests for shear walls and 12 dynamic tests for roofs. Ongoing research consists in improving numerical predictions at the scale of the house. In the future, it is intended to use this model as a tool to better understand the behavior of timber frame structures under seismic loading. It will also be possible to compare the results of a time-history analysis to the simplified design methods of the Eurocode 8 [1].

ACKNOWLEDGEMENT

The French Agency (ANR RiskNat 2008) is gratefully acknowledged. The authors would like to express their gratitude to all the members of the SISBAT research project, especially C. Faye (FCBA Technological Institut), P.E. Charbonnel, M. Chaudat (CEA) and their colleagues for the effort provided for the realization of the experimental campaign.

REFERENCES

- [1] EN 1998-1: Design of structures for earthquake resistance - General rules, seismic actions and rules for buildings, CEN, 2005.
- [2] Richard N., Daudeville L., Prion H., Lam F. Timber shear walls with large openings: experimental and numerical prediction of the structural behavior. *Canadian Journal of Civil Engineering*, 29:713-724, 2002.
- [3] Xu J., Dolan J.D. Development of a wood-frame shear wall in Abaqus, *Journal of Structural Engineering*, 135(8): 968-976, 2009.
- [4] Humbert J., Boudaud C., Baroth J., Hameury S., Daudeville L. Joints and wood shear walls modeling I: Constitutive law, experimental tests and FE model under quasi-static loading. *Engineering Structures*, 65: 52-61, 2014.
- [5] Bertil, D., Rey, J., & Belvaux, M. *Modélisation de l'action sismique. Rapport final*. BRGM/RP-58886-FR: Projet ANR SISBAT, 2010.
- [6] Ceccotti A., Vignoli. A pinching hysteretic model for semi-rigid joints, *European Earthquake Engineering Journal*, 3:3-9, 1989.
- [7] Folz B., Filiatrault A. Seismic analysis of wood-frame structures II: Model implementation and verification, *Journal of Structural Engineering*, 130(9): 1361-1370, 2004.
- [8] Richard N., Yasumura M., Davenne L.: Prediction of the seismic behavior of wood-framed shear walls with openings by pseudodynamic test and FE model, *Journal of Wood Science*, 49:145-151, 2003
- [9] Yasumura M.: Evaluation of the damping capacity of timber structures for seismic design, *Proceedings 34th CIB-W18*, 2001.
- [10] EN 12512. Timber Structures – Test methods – Cyclic testing on joints made with mechanical fasteners. 2002
- [11] Gupta A., Kuo G. Behavior of wood-framed shear walls. *Journal of Structural Engineering*, 111(8), 1722-1733, 1985
- [12] Dutil D., Symans M. Experimental investigation of seismic behavior of light-framed wood shear walls with supplemental energy dissipation. *Proc. 31th World Conference on Earthquake Engineering*, Paper No 3421.
- [13] Humbert J. Characterization of the behavior of timber structures with metal fasteners undergoing seismic loadings. PhD Thesis. Univ. Grenoble. 2010